Optical second-harmonic generation in lossy media: Application to GaSe and InSe

E. Bringuier and A. Bourdon
Acoustique et Optique de la Matière Condensée, Université Pierre et Marie Curie, Case 86, 4 place Jussieu, 75 252 Paris Cedex 05, France

N. Piccioli and A. Chevy
Physique des Milieux Condensés, Université Pierre et Marie Curie, Case 77, 4 place Jussieu, 75 252 Paris Cedex 05, France

(Received 18 January 1994)

The paper deals with optical second-harmonic generation in a medium absorbing the second-harmonic radiation, and where phase matching between the fundamental and second-harmonic radiation is not necessarily achieved. We first take the waves to be in the form of traveling waves, and describe the damping of the fundamental beam due to harmonic creation. It is found that both second-harmonic absorption and phase mismatch enhance the depletion length of the pump wave. Before depletion, the second-harmonic output power is independent of the traversed thickness if it exceeds the second-harmonic attenuation length. When depletion occurs, the second-harmonic output power is constant, instead of quadratic, in the input power. Next, second-harmonic generation in a plane-parallel plate of lossy material is envisaged in the case of normal incidence, including the multiple reflections expected in high-reflectance materials. The expressions of the harmonic output intensity, transmitted or reflected, of this paper and from the conventional treatment, are compared. The deviation is noticeable in the case of the transmitted harmonic power, and may be considerable in the case of the reflected power. Last, measurements of the second-harmonic output intensity in GaSe and InSe are reported at a fundamental wavelength of 1.06 μm. The sample dependence is in good agreement with our theory, which in turn is applied to derive new values of the nonlinear optical susceptibilities in the layered-structured III-VI materials. The treatment is fully analytical and may be applied to a wealth of materials.

I. INTRODUCTION

The layered-structured III-VI compounds GaSe and InSe have attracted much attention because of their very high nonlinear optical coefficients in the infrared (IR) range, making them candidates for second-harmonic (SH) generation.[1–4] In performing power measurements of the SH radiation generated in thin layers of both materials with a fundamental wavelength of 1.06 μm, we found[4] that the transmitted SH power was not very different between both selenides. Since the reported nonlinear susceptibility of GaSe is about fourfold that of InSe, and since SH absorption at 0.53 μm is higher in the latter material owing to its smaller band gap, the expected ratio in SH generation is expected to be at least 16 in favor of GaSe. This called for a closer examination of harmonic generation in such materials. The conventional treatment[5] of SH generation is restricted to the case of nonabsorbing media, or to the rarely relevant case of identical IR and SH absorption.[6] Furthermore, phase matching between the fundamental and SH radiation is often assumed. In GaSe and InSe, none of those simplifications can be made[7,8] for a fundamental wavelength of 1.06 μm: (i) the second-harmonic photon energy is higher than the band gap, so that SH and not IR is absorbed; and (ii) no phase matching at 1.06 μm was achieved so far. Since other materials[9] of physical or technological significance share one or both features, a general treatment of harmonic generation including SH absorption and phase mismatch is highly desirable. This is the purpose of the present paper, which is structured as follows. Section II is devoted to the generation of SH radiation due to a traveling IR wave in the presence of SH absorption and phase mismatch, including the depletion of the pump wave. The approach is analytical and outlines the relevant length scales associated with various possible behaviors (the detailed calculations are given in Appendix A). The results are applied to our materials. Section III considers SH generation in a plane-parallel plate of lossy material, including the multiple IR and SH reflections expected in high-reflectance materials (details in Appendix B). The expressions for the SH output intensity obtained in Secs. II and III and in previous studies are compared in Sec. IV, and experimental values of the second-order optical susceptibilities of GaSe and InSe are derived. Section V sketches the conclusions.

II. DAMPED SECOND-HARMONIC GENERATION

A. The propagation equations and the ideal case

The propagation equations for collinear sinsoidal waves at ω and 2ω, coupled by a nonlinear polarization that is proportional to the square of the field, were first obtained by Armstrong *et al.*[6] in the general form of sum-frequency conversion. Their application to SH generation ($\omega+\omega\rightarrow 2\omega$) has been reviewed by Craxton.[10] For the sake of clarity, we shall briefly recall the steps involved. If the harmonic electric field is written in the form $E_{2\omega}(z)\exp(2i\omega t)$, where z denotes the propagation

0163-1829/94/49(24)/16971(12)/$06.00 ©1994 The American Physical Society

coordinate, the spatial part $E_{2\omega}(z)$ is the solution of an inhomogeneous differential equation:

$$[d^2/dz^2+(k_{2\omega}-i\beta)^2]E_{2\omega}=-2\mu_0\omega^2 d' E_\omega^2 , \quad (1a)$$

where the source term (right-hand side) originates from the nonlinear polarization, and involves the spatial part of the electric field at ω, $E_\omega(z)$, and d' is a component of the (real) nonlinear susceptibility tensor in the coordinate system used to describe the propagation. We use mks units such that d'/ε_0 is in m/V. In Eq. (1a), $k_{2\omega}=n_{2\omega}(2\omega/c)$, $n_{2\omega}$, and β, respectively, are the wave vector, (real) refraction index, and attenuation coefficient at 2ω (β is half the energy absorption coefficient). Conversely, $E_\omega(z)$ is governed by a differential equation:

$$[d^2/dz^2+k_\omega^2]E_\omega=-\mu_0\omega^2 d' E_\omega^* E_{2\omega} , \quad (1b)$$

where the right-hand side describes the coupling with the SH wave, and $k_\omega=n_\omega(\omega/c)$ and n_ω, respectively, stand for the wave vector and the refraction index at ω. Since the magnitude of the harmonic wave is of order E_ω^2 at low E_ω, the right-hand side is often dropped at low power, so that the fundamental wave propagates unperturbed by SH generation. We shall *not* do so in this section. In what follows, the electric fields at ω and 2ω are taken to be in the form of traveling plane waves along increasing z, so that complex amplitudes $A_{n\omega}(z)$ may be defined from the $E_{n\omega}(z)$'s by extracting the usual traveling part:

$$E_\omega(z)=n_\omega^{-1/2}A_\omega(z)\exp(-ik_\omega z) , \quad (2a)$$

$$E_{2\omega}(z)=n_{2\omega}^{-1/2}A_{2\omega}(z)\exp(-ik_{2\omega}z-\beta z) . \quad (2b)$$

In Eq. (2b) the traveling term includes the SH attenuation factor. The reason for including this factor lies in the simplicity of the equations obeyed by the amplitudes $A_{n\omega}$ so defined. The prefactors in Eqs. (2a) and (2b) are such that the Poynting vectors at z may be written

$$P_\omega(z)=(\tfrac{1}{2})\varepsilon_0 c|A_\omega(z)|^2 , \quad (3a)$$

$$P_{2\omega}(z)=(\tfrac{1}{2})\varepsilon_0 c|A_{2\omega}(z)|^2\exp(-2\beta z) . \quad (3b)$$

The nonlinear medium is located at $0<z<d$. An incident wave at ω comes from vacuum ($z<0$), so that $P_\omega(0)$ (henceforth denoted as P_ω) defines $A_\omega(0)$ (real), while $A_{2\omega}(0)=0$. By $P_{2\omega}$ we shall denote $P_{2\omega}(d)$, which will be called the SH output power density.

Next, we make the approximation of slowly varying amplitudes; that is, the variation of the complex field amplitudes with z is small enough that

$$k_\omega|dA_\omega/dz|\gg|d^2A_\omega/dz^2| , \quad (4a)$$

$$|(k_{2\omega}-i\beta)dA_{2\omega}/dz|\gg|d^2A_{2\omega}/dz^2| . \quad (4b)$$

If $\beta<k_{2\omega}$, the second condition entails

$$k_{2\omega}|d[A_{2\omega}\exp(-\beta z)]/dz| \gg |d^2[A_{2\omega}\exp(-\beta z)]/dz^2| . \quad (4c)$$

After that change of variables and this approximation have been made, for $\beta\ll k_{2\omega}$ we obtain

$$dA_\omega/dz=-i\kappa A_\omega^* A_{2\omega}\exp(-\Lambda z) , \quad (5a)$$

$$dA_{2\omega}/dz=-i\kappa A_\omega^2\exp(\Lambda z) , \quad (5b)$$

where $\Lambda=\beta+i\Delta k$, and $\Delta k=k_{2\omega}-2k_\omega$ is the phase mismatch; the coherence length is defined as $1/\Delta k$. We have recovered Eqs. (A9) and (A10) of Ref. 10. The coefficient κ is related to the nonlinear susceptibility d' through[10]

$$\kappa=\frac{\omega}{2c}(n_\omega^2 n_{2\omega})^{-1/2}\frac{d'}{\varepsilon_0} . \quad (6)$$

Table I lists the material parameters[1,7,8] for GaSe and InSe. The linear coefficients have been obtained by our group,[7,8] and the nonlinear susceptibilities are taken from Akhundov *et al.*[1] We call $|\Lambda|^{-1}=(\beta^2+\Delta k^2)^{-1/2}$ the "attenuation-coherence length," which is of the order of the smaller of the coherence length Δk^{-1} and the attenuation length β^{-1}. $\Lambda=0$ will be referred to as the ideal case, which has already received solution.[5] The picture obtained in the ideal case may be described either in terms of length (at constant incoming power) or power (at constant traversed thickness). There appears a characteristic length l,

$$l=\kappa^{-1}(2P_\omega/\varepsilon_0 c)^{-1/2} , \quad (7)$$

over which the fundamental wave is converted into SH. For sample thickness $d\gg l$, the input power at ω is entirely converted into SH. The conversion is complete due to phase matching, and lossless due to a lack of absorption. Increasing the input power density P_ω shrinks the typical conversion length l as $(P_\omega)^{-1/2}$: for a high enough input power, l becomes $\ll d$ and all IR light is converted into SH. Now in terms of power at constant d, the $P_{2\omega}(P_\omega)$ relationship begins quadratically and saturates to the asymptotic law $P_{2\omega}=P_\omega$:

$$P_{2\omega}=P_\omega\{\tanh[\kappa d(2P_\omega/\varepsilon_0 c)^{1/2}]\}^2 . \quad (8)$$

TABLE I. Material parameters (fundamental wavelength in vacuum $=1.06\ \mu$m). The linear constants have been measured by our group (Refs. 7 and 8); the nonlinear coefficient is taken from Ref. 1, with $d'/\varepsilon_0=5.6\times10^{-13}$ m/V for KDP.

	Refraction index at ω n_ω	Refraction index at 2ω $n_{2\omega}$	Coherence length $1/\Delta k$ (μm)	Attenuation length β^{-1} (μm)	Relative attenuation $\beta/k_{2\omega}$	Nonlinear coefficient κ (V^{-1})
GaSe	2.800	3.068	0.315	10	2.7×10^{-3}	2.32×10^{-4}
InSe	2.788	3.210	0.200	2	1.3×10^{-2}	0.505×10^{-4}

The highest powers investigated in Ref. 4 ($P_\omega \sim 10^9$ W/cm^2) yield l of the order of sample thickness d, so that an exact calculation including the nonideal effects (SH absorption, phase mismatch) is necessary.

B. The nonideal case

Now, what will happen in the nonideal case? Both phase mismatch and absorption tend to lengthen the characteristic scale over which the fundamental wave will be converted into SH radiation. First, part of the energy at 2ω is sent back to the fundamental mode due to mismatch. Second, the 2ω wave is damped, which decreases the energy exchange between both modes. Hence, if the effects of mismatch and absorption take place over a characteristic length $|\Lambda|^{-1}$ shorter than the ideal IR-SH conversion length l (Table II), we can expect the damping of the fundamental wave to occur over very large lengths for nonzero Λ, thereby allowing us to integrate Eq. (5b) by parts while neglecting dA_ω/dz:

$$A_{2\omega}(z)=(-i\kappa/\Lambda)[A_\omega^2(z)\exp(\Lambda z)-A_\omega^2(0)] , \tag{9a}$$

or, equivalently,

$$A_{2\omega}(z)\exp(-\beta z)=(-i\kappa/\Lambda)[A_\omega^2(z)\exp(i\Delta kz) - A_\omega^2(0)\exp(-\beta z)] , \tag{9b}$$

taking as initial conditions $A_\omega(0)$ real, and $A_{2\omega}(0)=0$.

In (9b) the real exponential quickly decays for $z \gg \beta^{-1}$. The first term on the right-hand side of (9b) decreases as the square modulus of the ω wave, i.e., on distances of l (in the ideal case) or more (in the nonideal one), very slowly compared to the phase term $\exp(i\Delta kz)$, which varies over the much shorter coherence length $1/\Delta k$. In this paper, we consider the case where l is longer than the attenuation-coherence length $|\Lambda|^{-1}$. If this condition [allowing the writing of (9)] is not fulfilled, it means that the fundamental could be converted into second-harmonic radiation before absorption and phase mismatch have appreciable effects. This is highly unrealistic given our material parameters, with $|\Lambda|^{-1}$ around the μm. Furthermore, the amplitude A_ω would then vary over such short scales that neither the integration by parts leading to (9) nor the approximation of slowly varying amplitudes would be valid. Practically speaking, the condition $l > |\Lambda|^{-1}$, viz.

$$P_\omega < (\tfrac{1}{2})\varepsilon_0 c|\Lambda|^2\kappa^{-2} , \tag{10}$$

breaks down for a huge incoming power.

In the case where $l \gg |\Lambda|^{-1}$, injecting (9a) into (5a) gives a differential equation on the sole function A_ω:

$$dA_\omega/dz=-(\kappa^2/\Lambda)A_\omega^*[A_\omega^2(z)-A_\omega^2(0)\exp(-\Lambda z)] , \tag{11}$$

which can be solved by separate examination of the modulus and phase of $A_\omega(z)$. The detailed calculation of $A_\omega(z)$ and $A_{2\omega}(z)$ can be found in Appendix A, and here we just sketch the main results, emphasizing the role of length scales.

(i) The amplitude $|A_\omega(z)|$ of the fundamental is now governed by *two* characteristic lengths, namely $|\Lambda|^{-1}$ and L,

$$L=(|\Lambda|^2/2\beta)l^2=[\varepsilon_0 c/(4P_\omega\kappa^2)](\Delta k^2+\beta^2)/\beta , \tag{12}$$

instead of *one* length, the typical IR-SH conversion scale l, in the ideal case. Note that L depends on the input power density as P_ω^{-1}. Because $l \gg |\Lambda|^{-1}$, we have the following chain of inequalities (see Table II):

$$L \gg l \gg |\Lambda|^{-1} .$$

For fixed P_ω and finite Δk, L increases as $\beta \to 0$: for low SH absorption, there is hardly any decay of the pump wave. For fixed P_ω and $\Delta k=0$, the depletion length of the ω wave in the presence of SH absorption $L=\beta l^2/2$ is longer than the ideal one, since $\beta l \gg 1$: this apparently counterintuitive result is due to the fact that the weakening of the 2ω wave over a length $\beta^{-1} \ll l$ lowers the rate of (coherent) SH creation. Finally, we note that the integration by parts yielding (9) is justified, since $L \gg |\Lambda|^{-1}$.

(ii) Near $z=0$, the second-harmonic amplitude $|A_{2\omega}(z)|$ varies as $|1-e^{-\Lambda z}|$: it is pseudoperiodic, the oscillations being damped for $z \gg \beta^{-1}$. Thereafter $|A_{2\omega}(z)|$ is flat as long as z stays between β^{-1} and L. At last, for $z > L$, $|A_{2\omega}(z)|$ smoothly decreases as $(1+z/L)^{-1}$, corresponding to the damping of the fundamental wave. Where $\beta^{-1} \ll z \ll L$, the harmonic wave is continuously absorbed, but at the same time continuously regenerated by the ω wave, which eventually dies for $z \gg L$. The optimum thickness for SH generation lies between $z=\pi/2\Delta k$ and $\pi/\Delta k$, accordingly, as $\beta \gg$ or $\ll \Delta k$, after which the output power reaches a stable value within some attenuation lengths. Figure 1 gives a graphical representation of $|A_{2\omega}(z)|^2$. The behavior of the phases of functions A_ω and $A_{2\omega}$ is described in Appendix functions A_ω and $A_{2\omega}$ is described in Appendix A.

Now what is the SH output power density $P_{2\omega}$ when the incoming power density P_ω and the thickness d are varied? First, keeping P_ω fixed, we vary d. For $d \ll L$, $P_{2\omega}$ varies quadratically in P_ω, and for $d \gg L$, $P_{2\omega}$ becomes independent of the input power. Second, keeping d fixed, we vary P_ω. As long as $L \sim P_\omega^{-1}$ remains larger than d, then $(1+d/L)^{-2} \simeq 1$, and $P_{2\omega}$ varies as P_ω^2:

$$P_{2\omega}=[\kappa^2/(\Delta k^2+\beta^2)](2P_\omega^2/\varepsilon_0 c) \quad (d \gg \beta^{-1}) , \tag{13a}$$

which is to be multiplied by $|1-\exp(-\Lambda d)|^2$ if d is of the order of β^{-1}. At high enough input power, $L \le d$, and $P_{2\omega}$ varies subquadratically in P_ω and eventually becomes constant:

TABLE II. The relevant length scales at $P_\omega = 10^9$ W/cm^2 ($l \sim P_\omega^{-1/2}$, $L \sim P_\omega^{-1}$).

	Attenuation-coherence length $\|\Lambda\|^{-1}$ (μm)	Ideal conversion length $l(P_\omega)$ (μm)	Nonideal damping length $L(P_\omega)$ (cm)
GaSe	0.315	49.6	12.4
InSe	0.199	228	131

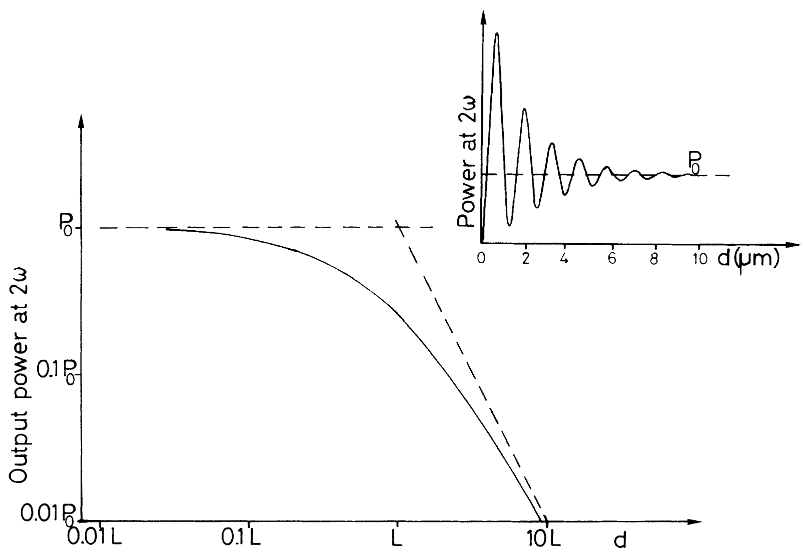

FIG. 1. Calculated output power at 2ω in the case of pure traveling waves, as a function of the traversed thickness d, in logarithmic scales. For $d \ll L$, $P_{2\omega}=P_0$ given by Eq. (13a); for $d \gg L$, $P_{2\omega} \sim d^{-2}$ is given by Eq. (13b). The oscillations in the growth of $P_{2\omega}$ for very small thicknesses ($\beta d \lesssim 1$) have been drawn in the inset (with InSe parameters): for $\beta d \gg 1$, $P_{2\omega}=P_0$.

$$P_{2\omega}=(\tfrac{1}{2})\varepsilon_0 c\,|\Lambda|^2/(2\kappa\beta d)^2 \ , \tag{13b}$$

whatever the input power. Figure 2 displays the crossover between both behaviors, taking GaSe as an example. This is in contrast to the ideal case[5] ($\Lambda=0$), where at low power $P_{2\omega} \sim P_\omega^2$ and at high enough power $P_{2\omega} \simeq P_\omega$. For convenience the ideal SH response is also displayed in Fig. 2.

In the case of GaSe and InSe, the characteristic length L beyond which SH generation is subquadratic is very large in spite of the high nonlinear coefficients κ. Therefore we may consider that (i) the SH output power is always quadratic in input IR power, and (ii) the fundamental wave is undamped in the practical range of thicknesses available. Most of the markedly nonideal materials will in fact keep in the quadratic regime. In that regime for thick enough layers ($d \gg \beta^{-1}$) the reduction in output power compared to the ideal case is equivalent

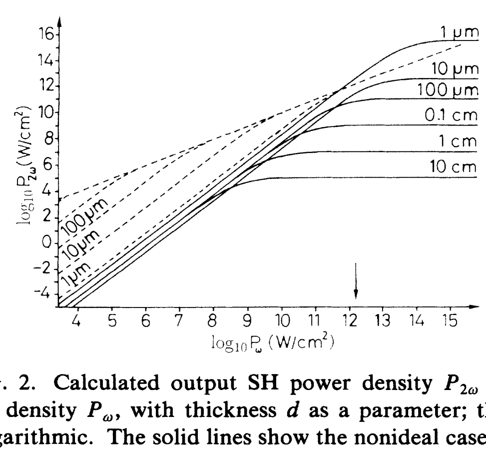

FIG. 2. Calculated output SH power density $P_{2\omega}$ vs input power density P_ω, with thickness d as a parameter; the scales are logarithmic. The solid lines show the nonideal case, and the dashed lines the ideal case ($\Lambda=0$), with GaSe parameters (Table I). The upper power limit for the treatment of Sec. II to be valid, corresponding to $l=|\Lambda|^{-1}$, has been indicated by an arrow on the incident power axis. Note that for short thicknesses ($\beta d \lesssim 1$), the prefactor $|1-e^{-\Lambda d}|^2$ deviates from its asymptotic value (unity) and varies between 0 and 4.

to replacing d by $|\Lambda|^{-1}$ in Eq. (8). Hence as far as harmonic conversion efficiency is concerned, a nonideal material is equivalent to an ideal material having the same nonlinear coefficient κ with a thickness equal to the attenuation-coherence length.

III. THE PLANE-PARALLEL PLATE

Section II has shown that in the practical ranges of power and thickness, the damping of the fundamental wave could be neglected. Then the output harmonic power is quadratic in IR power and given by Eq. (13a). The calculation has been done in the slowly varying amplitude approximation, and with the assumption of forward traveling waves at ω and 2ω. In this section we shall lift those two restrictions. This is needed since (i) our selenide samples are plane-parallel plates of high reflectance both at ω and 2ω (Table I), leading to nonnegligible standing-wave ratios; and (ii) in InSe the attenuation length is of the order of the wavelength in the medium. The treatment of Bloembergen and Pershan[11] was limited to a low reflectance at ω. We will therefore return to the general propagation equation (1a) governing the spatial part $E_{2\omega}(z)$ of the electric field at 2ω, that we rewrite here for convenience:

$$[d^2/dz^2+(k_{2\omega}-i\beta)^2]E_{2\omega}=-2\mu_0\omega^2 d' E_\omega(z)^2 \ . \tag{14}$$

According to Sec. II, $E_\omega(z)$ is negligibly affected by SH generation, and can be derived from the linear propagation theory. Consequently for $E_\omega(z)$ we take a superposition of forward- and backward-traveling waves:

$$E_\omega(z)=E_0\{\exp(-ik_\omega z)+r\exp[ik_\omega(z-d)]\} \ , \tag{15}$$

where E_0 is related to the incident wave field $E_{\rm in}$ at ω in vacuum arriving from the left at $z=0$ through the well-known Fresnel formulas:

$$E_0=\frac{2E_{\rm in}/(n_\omega+1)}{1-R_\omega \exp(-2ik_\omega d)} \ , \tag{16a}$$

$$r = R_\omega^{1/2}\exp(-ik_\omega d)\ , \quad R_\omega = [(n_\omega - 1)/(n_\omega + 1)]^2\ , \tag{16b}$$

where d is the plate thickness, which occupies the space $0 < z < d$, and R_ω denotes the energy reflection coefficient at ω. Absorption of the fundamental wave (not considered here) would not alter the treatment, and a negative imaginary part would just be added to k_ω in Eqs. (15) and (16).

When expression (15) is substituted into Eq. (14), solving for (14) is straightforward. The right-hand side of (14) gives rise to a forced harmonic wave:

$$E_{2\omega}(z) = -2\mu_0\omega^2 d' E_0^2 \left\{ \frac{\exp(-2ik_\omega z) + r^2\exp[2ik_\omega(z-d)]}{(k_{2\omega} - i\beta)^2 - (2k_\omega)^2} + \frac{2r\exp(-ik_\omega d)}{(k_{2\omega} - i\beta)^2} \right\} . \tag{17}$$

The wave is forced in the sense that its wave vector $2k_\omega$ is determined by the source wave at ω. In (17) there are two traveling waves (along $+z$ and $-z$) and a constant term. In the case of weak loss ($\beta \ll k_{2\omega}$), a resonance appears for $k_{2\omega} = 2k_\omega$, i.e., when the forced wave vector $2k_\omega$ is matched to the free wave vector $k_{2\omega}$. The response $E_{2\omega}$ at resonance is limited only by the losses at 2ω. In the absence of any linear loss (that is, $\beta = 0$), a particular solution of Eq. (14) for $k_{2\omega} = 2k_\omega$ is

$$E_{2\omega}(z) = -2\mu_0\omega^2 d' E_0^2 \frac{i}{2k_{2\omega}} (z\{\exp(-ik_{2\omega}z) - r^2\exp[ik_{2\omega}(z-d)]\} - 4ir\exp(-ik_\omega d)/k_{2\omega}) . \tag{18}$$

As $|r| < 1$, this is essentially a forward-traveling wave whose amplitude grows with z: we recover the usual case[5] of coherent (i.e., phase matched), lossless SH generation. It turns out that the standing-wave ratio of the SH wave equals that of the fundamental wave, as follows from index matching at ω and 2ω. In what follows this case is discarded.

To the particular solution (17) of Eq. (14) we may add any solution of the homogeneous equation, that is, free waves propagating with the free wave vector $k_{2\omega}$ and attenuated over a length β^{-1}:

$$b_+\exp[-(ik_{2\omega}z + \beta)z] + b_-\exp[(ik_{2\omega} + \beta)(z-d)] . \tag{19}$$

The signification of the free waves is clear[11] if one notices that the constants b_+ and b_- are determined by the boundary conditions at $z = 0$ and d. At the boundaries, the harmonic wave gives rise to SH radiation in vacuum:

$$E_{2\omega}(z) = E_{\text{out}}\exp[-2i\omega(z-d)/c] \quad (z > d)\ , \tag{20a}$$

$$E_{2\omega}(z) = E'_{\text{out}}\exp(2i\omega z/c) \quad (z < 0)\ . \tag{20b}$$

The wave (20a) propagating along $+z$ is usually called the harmonic transmitted wave, while the wave (20b) traveling along $-z$ is the so-called harmonic reflected wave. The need to satisfy two continuity conditions (electric and magnetic) calls for the presence of a free wave at 2ω inside the plate of the form (19).

In Ref. 11 those conditions were expressed for arbitrary incidence of the pump beam, but the reflectance at ω was supposed to be small ($r \simeq 0$). Then the SH electric fields in vacuum for transmission (E_{out}) and reflection (E'_{out}) were expressed as functions of the nonlinear source term. Those formulas were used in various determinations of nonlinear coefficients in lossy materials. In our materials the indices are high, making the simplification of small reflectance unacceptable, so we embark on a general calculation for arbitrary r. The calculation is detailed in Appendix B, taking the attenuation length to be $\ll d$. This is the interesting case in view of our material parameters (Table I). The opposite case ($\beta d \lesssim 1$) yields very complicated expressions.

Introducing the complex optical index at 2ω, of which the imaginary part β' is *minus* the relative attenuation coefficient (attenuation over the reduced SH wavelength in vacuum):

$$\tilde{n}_{2\omega} = n_{2\omega} - i\beta'\ , \quad \beta' = \beta c/2\omega\ , \tag{21}$$

the forward-traveling (transmitted) field at 2ω in vacuum is given by

$$E_{\text{out}} = -\frac{d'}{2\varepsilon_0}\frac{[2E_{\text{in}}\exp(-ik_\omega d)/(n_\omega + 1)]^2}{[1 - R_\omega\exp(-2ik_\omega d)]^2(\tilde{n}_{2\omega} + 1)} \times \left\{ \frac{\tilde{n}_{2\omega}(1 + R_\omega) + n_\omega(1 - R_\omega)}{\tilde{n}_{2\omega}^2 - n_\omega^2} + \frac{2R_\omega^{1/2}}{\tilde{n}_{2\omega}} \right\} . \tag{22a}$$

The reflected field at 2ω is given by a similar expression:

$$E'_{\text{out}} = -\frac{d'}{2\varepsilon_0}\frac{[2E_{\text{in}}\exp(-ik_\omega d)/(n_\omega + 1)]^2}{[1 - R_\omega\exp(-2ik_\omega d)]^2(\tilde{n}_{2\omega} + 1)} \times \left\{ \frac{\tilde{n}_{2\omega}[1 + R_\omega\exp(-4ik_\omega d)] - n_\omega[1 - R_\omega\exp(-4ik_\omega d)]}{\tilde{n}_{2\omega}^2 - n_\omega^2} + \frac{2R_\omega^{1/2}\exp(-2ik_\omega d)}{\tilde{n}_{2\omega}} \right\} . \tag{22b}$$

Expressions (22a) and (22b) are valid for $\beta d \gg 1$. The limiting case of pure traveling waves treated in Sec. II may be obtained from the present expression for the transmitted field by taking $n_{2\omega} \simeq 1$ and $n_{\omega} \simeq 1$, corresponding to small reflectances, together with a not too high attenuation coefficient at 2ω (i.e., $\beta' < 1$) owing to the slowly varying amplitude approximation made in Sec. II. In other words, Eq. (22a) yields the result of Sec. II if we let the complex indices at ω and 2ω tend toward unity. The quantitative comparison between the transmitted SH powers in our materials given by various treatments is the subject of Sec. IV.

The modulus of each outgoing harmonic field is modulated according to the plate thickness, reminiscent of the standing-wave ratio of the fundamental wave. The modulation depth is an increasing function of the reflection coefficient R_{ω}. The square modulus of each outgoing field is proportional to

$$f(d)=\left\{(1+R_{\omega}^2)\left[1-\frac{2R_{\omega}}{1+R_{\omega}^2}\cos(2k_{\omega}d)\right]\right\}^{-2} . \tag{23a}$$

That thickness-dependent factor is to be replaced by an average value if thickness fluctuations exceed the fundamental wavelength. The average value of (23a) involves an elliptic integral of which a limited expansion is

$$\langle f\rangle=(1+R_{\omega}^2)^{-2}\left[1+(\tfrac{3}{2})\left[\frac{2R_{\omega}}{1+R_{\omega}^2}\right]^2+(\tfrac{15}{8})\left[\frac{2R_{\omega}}{1+R_{\omega}^2}\right]^4+\cdots\right] . \tag{23b}$$

That expansion is sufficient even in our highly reflective materials.

The transmitted and reflected SH power densities $P_{2\omega}$ and $P'_{2\omega}$, respectively, are

$$P_{2\omega}=(2P_{\omega}^2/\varepsilon_0 c)(d'/\varepsilon_0)^2 f(d)[2/(n_{\omega}+1)]^4\frac{1}{4|\tilde{n}_{2\omega}+1|^2}\left|\left\{\frac{\tilde{n}_{2\omega}(1+R_{\omega})+n_{\omega}(1-R_{\omega})}{\tilde{n}_{2\omega}^2-n_{\omega}^2}+\frac{2R_{\omega}^{1/2}}{\tilde{n}_{2\omega}}\right\}\right|^2 \tag{24a}$$

$$P'_{2\omega}=(2P_{\omega}^2/\varepsilon_0 c)(d'/\varepsilon_0)^2 f(d)[2/(n_{\omega}+1)]^4 4^{-1}|\tilde{n}_{2\omega}+1|^{-2}$$
$$\times\left|\left\{\frac{\tilde{n}_{2\omega}[1+R_{\omega}\exp(-4ik_{\omega}d)]-n_{\omega}[1-R_{\omega}\exp(-4ik_{\omega}d)]}{\tilde{n}_{2\omega}^2-n_{\omega}^2}+\frac{2R_{\omega}^{1/2}\exp(-2ik_{\omega}d)}{\tilde{n}_{2\omega}}\right\}\right|^2 , \tag{24b}$$

where $f(d)$ is given by (23).

IV. DISCUSSION

A. Comparison between theories

This subsection is devoted to comparing the expressions for the SH output power density obtained in this paper [Eqs. (13) and (24a)], together with the expression of Bloembergen and Pershan.[11] Section IV B describes the experimental behavior of the SH output power in GaSe and InSe, and this is applied to the practical determination of d' in our materials, which so far[1–3] referred to Bloembergen and Pershan's treatment.[11]

To compare the various theoretical expressions for the density of SH output power we write them on the pattern,

$$P_{2\omega}=(2P_{\omega}^2/\varepsilon_0 c)(d'/\varepsilon_0)^2\phi , \tag{25}$$

so that they differ in the dimensionless factor ϕ containing the complex refraction indices. The treatment of Sec. II [Eq. (13)] yields

$$\phi=\{16n_{\omega}^2 n_{2\omega}[(n_{2\omega}-n_{\omega})^2+\beta'^2]\}^{-1} , \tag{26}$$

while that of Sec. III [Eq. (24a)] has a ϕ:

$$\phi=f(d)\left[\frac{2}{n_{\omega}+1}\right]^4\frac{1}{4|\tilde{n}_{2\omega}+1|^2}$$
$$\times\left|\left\{\frac{\tilde{n}_{2\omega}(1+R_{\omega})+n_{\omega}(1-R_{\omega})}{\tilde{n}_{2\omega}^2-n_{\omega}^2}+\frac{2R_{\omega}^{1/2}}{\tilde{n}_{2\omega}}\right\}\right|^2 . \tag{27}$$

Equations (26) and (27) coincide when both complex refraction indices approach unity: the asymptotic expression for ϕ is then

$$\phi\sim\{16[(n_{2\omega}-n_{\omega})^2+\beta'^2]\}^{-1} . \tag{28}$$

That limiting case corresponds to approximate phase matching and vanishing SH loss per unit length over a very thick plate, since $d \gg \beta^{-1}$. Equation (28) provides an easy way to check the results given by different frameworks.

In the thickness range where the fundamental wave is not depleted, and for $d \gg \beta^{-1}$, the difference between Secs. II and III is twofold: (i) the assumption of slowly varying amplitudes is not used in Sec. III; and (ii) exact boundary conditions at ω and 2ω are used in Sec. III, thereby accounting for the internal reflections occurring in a plane-parallel plate. Table I shows that the approximation of slowly varying amplitude is good in GaSe at 1.06 μm, while it might be questioned in InSe in regard of its violent attenuation. As a matter of fact the approximation of slowly varying amplitudes consists in dropping the β'^2 term in the resonant denominator of Eqs. (22a) and (22b). In view of the smallness of $\beta'/n_{2\omega}$ (see Table I), the error introduced by that approximation is insignificant in either material. Hence the practical difference between the two treatments is essentially due to the boundary conditions.

The difference associated with the boundary conditions in (26) and (27) is twofold. The most obvious one lies in the Fresnel relationship (16) between the internal field E_ω and the field in vacuum $E_{\rm in}$, and is expressed by the product of $[2/(n_\omega+1)]^4$ by $f(d)$ arising from the multiple reflections. In both materials $\langle f \rangle$ little departs from unity: $\langle f \rangle = 1.213$ (GaSe) and 1.208 (InSe). The $[2/(n_\omega+1)]^4$ term is significantly lower than unity (0.077 in GaSe and 0.078 in InSe). The second difference comes from the treatment of the boundary conditions for the *harmonic* field, for which no obvious picture can be given (Appendix B). The factors ϕ are computed and listed in Table III, where $f(d)$ was replaced by its average $\langle f \rangle$. It is seen that the exact one is about two-thirds of the approximate one from Sec. II.

The treatment of Ref. 11 is intermediate between those of Secs. II and III, in that is supposes the reflectance at ω to be small. The field E_ω in the plate is considered to be that of a forward-traveling wave, i.e., $r \simeq 0$ in (15), and E_0 in (16a) may be written as $2E_{\rm in}/(n_\omega+1)$. In other words the standing-wave ratio is neglected. For normal incidence and a sufficiently thick plate (that is, $d \gg \beta^{-1}$), their Eq. (6.8) giving the transmitted harmonic field $E_{\rm out}$ simplifies to

$$E_{\rm out} = -4\pi\chi \left[\frac{2E_{\rm in}/\sqrt{2}}{n_\omega+1} \right]^2 \frac{1}{(\tilde{n}_{2\omega}+1)^2} \frac{\tilde{n}_{2\omega}^2+2\tilde{n}_{2\omega}+n_\omega}{\tilde{n}_{2\omega}^2-n_\omega^2} . \tag{29}$$

Equation (29) is written in the cgs-esu system. Note that we have replaced $E_{\rm in}$ by $E_{\rm in}/\sqrt{2}$: this is because the treatment of Refs. 6 and 11 deals with sum-frequency conversion instead of second-harmonic generation. When the frequencies of the incident beams coincide ($\omega+\omega \rightarrow 2\omega$), one should consider that two identical beams of power $P_\omega/2$ interact to yield a wave at 2ω, as has been shown in detail by Craxton.[10] The Poynting vector $P_{2\omega}$ associated with (29) is $(c/8\pi)|E_{\rm out}|^2$, and the mks formula is obtained from the cgs-esu one through the substitutions[12]

$$(4\pi)^2 \rightarrow 1/4\pi\varepsilon_0 , \quad \chi \rightarrow d'/\varepsilon_0 , \tag{30}$$

yielding the pattern (25) in which

$$\phi = \frac{1}{4} \left[\frac{2}{n_\omega+1} \right]^4 \left| \frac{\tilde{n}_{2\omega}^2+2\tilde{n}_{2\omega}+n_\omega}{(\tilde{n}_{2\omega}+1)^2(\tilde{n}_{2\omega}^2-n_\omega^2)} \right|^2 . \tag{31}$$

If we let n_ω and $\tilde{n}_{2\omega}$ approach unity, we do find the asymptotic form (28) for ϕ. If the values of ϕ are computed out of (31), we find that they are approximately half the exact ones; see Table III. Hence the formula of Ref. 11 underestimates the SH transmitted power, while Eq. (13) or (26) leads to an overestimation.

For the sake of completeness we also compare our predictions for the *reflected* harmonic power with those of Ref. 11. (The treatment of Sec. II is not considered, since it was based upon pure forward-traveling waves.) The power density $P'_{2\omega}$ of Sec. III may be cast in the form (25), with

$$\phi = f(d) \left[\frac{2}{n_\omega+1} \right]^4 \frac{1}{4|\tilde{n}_{2\omega}+1|^2} \times \left| \left\{ \frac{\tilde{n}_{2\omega}[1+R_\omega \exp(-4ik_\omega d)] - n_\omega[1-R_\omega \exp(-4ik_\omega d)]}{\tilde{n}_{2\omega}^2-n_\omega^2} + \frac{2R_\omega^{1/2}\exp(-2ik_\omega d)}{\tilde{n}_{2\omega}} \right\} \right|^2 \tag{32}$$

according to our Eq. (24b), and

$$\phi = \frac{1}{4} \left[\frac{2}{n_\omega+1} \right]^4 \left| \frac{1}{(\tilde{n}_{2\omega}+1)(\tilde{n}_{2\omega}+n_\omega)} \right|^2 \tag{33}$$

according to Eq. (6.7) of Ref. 11 [same steps as in deriving Eqs. (29) and (31)]. Equation (33) may be obtained from (32) by letting $R_\omega = 0$. The ϕ's are computed and given in Table IV, where for definiteness we have taken $\exp(-2ik_\omega d) = +$ or -1 in (32). The discrepancy between the reflected SH powers given by both formulas is more pronounced than that between the transmitted SH powers $P_{2\omega}$. This means that multiple reflections significantly increase the reflected SH power, so that the small-reflectance approximation can be in error by almost two orders of magnitude for SH generation by reflection in our materials.

Our treatment shows that both transmitted and reflected SH amplitudes are enhanced by multiple internal reflections. The reason lies in the Fabry-Pérot effect enhancing the fundamental field, and in the harmonic field being quadratic in the fundamental field. This is

TABLE III. The dimensionless prefactor ϕ for the transmitted SH power density according to various theories (Sec. II; Sec. III with $f(d) = \langle f \rangle$; and Ref. 11).

ϕ	Eq. (26) (Sec. II)	Eq. (27) (exact)	Eq. (31) (after Ref. 11)
GaSe	3.6×10^{-2}	2.3×10^{-2}	0.96×10^{-2}
InSe	1.4×10^{-2}	0.94×10^{-2}	0.37×10^{-2}

TABLE IV. The dimensionless prefactor ϕ for the reflected SH power density according to various theories [Sec. III of the present paper, and Eq. (6.7) of Ref. 11].

ϕ	Eq. (32) (exact) $\cos(2k_\omega d) = +1$	Eq. (32) (exact) $\cos(2k_\omega d) = -1$	Eq. (33) (after Ref. 11)
GaSe	5.5×10^{-3}	2.5×10^{-5}	3.4×10^{-5}
InSe	2.9×10^{-3}	7.9×10^{-5}	3.1×10^{-5}

most apparent in the thickness-dependent term $f(d)$ [Eq. (23)], which is a Fabry-Pérot interference function. If the cavity length is a multiple of a half-wavelength in the medium at ω, this leads to a high E_ω and a concomitant high SH output. With our figures $f(d)$ varies (around $\langle f \rangle = 1.2$) between 2.75 and 0.45, according to whether $\cos(2k_\omega d)$ equals $+$ or -1, i.e, with a period $\pi/k_\omega = 0.19$ μm.

B. Experiment

As far as we are aware, two previous experimental determinations of the nonlinear coefficients d' in GaSe and InSe at 1.06 μm have been published. Akhundov *et al.*[1] obtained values for d' by measuring the reflected SH power without giving information about their samples. Catalano and co-workers[2,3] made transmitted SH power measurements, and refer to Eq. (6.8) of Bloembergen and Pershan,[11] here rewritten as Eq. (31). Owing to the difficulty inherent in absolute determinations,[12] both groups made a relative determination of d' by comparing the SH output intensity from a GaSe or InSe sample to the one generated by a crystal of known nonlinear susceptibility. Table V lists the values obtained. In the case of Catalano and co-workers,[2,3] only *one* sample thickness d was used for each semiconductor, and we shall see further that this parameter plays a more important role in the determination of d' than previously assumed.

Our samples were grown in one of our laboratories by the vertical Bridgman transport method. An undoped GaSe crystal has been cleaved to form a set of thin GaSe platelets, the thicknesses d of which have been measured with an IR transmission spectrometer working around 3 μm. Only slices exhibiting a uniform thickness, evidenced by a high contrast, have been kept. Assuming a Gaussian distribution for d, the contrast may be related to the thickness standard deviation, and we find standard deviations ranging from 0.10 to 0.21 μm (unrelated to the thickness). Since the measurement is made with the relatively broad beam of the interferometer, it gives an upper limit of the thickness dispersion over the laser beam cross section. The values of d range from 1.5 to 518 μm, except for one very thick sample ($d \approx 1000$ μm). (Note that the range of thicknesses investigated extends down to $\beta d \lesssim 1$.) We did the same to make up a set ($15.8 \le d \le 243$ μm) of undoped InSe samples from only one ingot. All samples were mounted on a rotating sample holder so that the laser beam hit the sample normally onto a fixed 0.2-mm-diameter spot.

We used a Q-switched mode-locked Nd:YAG (yttrium aluminum garnet) laser which provided bursts of about 40 pulses at 1.06 μm. For each sample the incident IR power was varied from a maximum peak power of about

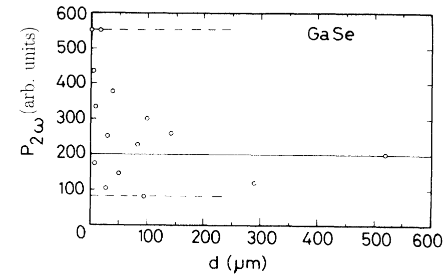

FIG. 3. Transmitted harmonic power output $P_{2\omega}$ as a function of traversed thickness d in GaSe, at constant incoming IR power. The dashed lines show the upper and lower limits of $P_{2\omega}$ due to the Fabry-Pérot cavity effect enhanced by laser instability [Eq. (34)]. The solid line indicates the expected output power for a sufficiently rough plate.

10^6 W. The output SH beam was separated from the transmitted IR beam by an interferential beam splitter. Its average power value $P_{2\omega}$ was recorded together with the average IR power P_ω. Along the IR power range investigated, we found a quadratic dependence of $P_{2\omega}$ versus P_ω within an experimental uncertainty arising from laser instability. It is normal that no subquadraticity be observed since d is much smaller than L; see Sec. II and Table II.

The slope $P_{2\omega}/P_\omega^2$ was found to depend rather randomly on sample thickness for both selenides, as shown on Figs. 3 and 4. The slopes exhibit a wide variation, especially for the thinner samples. This is consistent *only* with the prediction of Sec. III about Fabry-Pérot effects in second-harmonic generation. At first sight, these effects seem to bring a large uncertainty in the inferred value of d', but we shall show that one can take profit of them to provide a precise value of d'. These Fabry-Pérot effects were not taken into account by the aforementioned groups.

The $f(d)$ term in Eq. (23a) gives a ratio of 6.21 and 6.13 for GaSe and InSe, respectively, between the maxima and minima of $P_{2\omega}$ at constant P_ω. It should be stressed that $f(d)$ switches from a maximum to a minimum as d changes by $\pi/2k_\omega < 0.10$ μm, which is the typical thickness measurement accuracy of our samples. Therefore we can predict that a large enough assortment of thicknesses will yield a dynamic range of SH output power of 6.21 and 6.13. Indeed Figs. 3 and 4 give a maximum-to-minimum ratio of 6.88 and 7.78 for GaSe and InSe, respectively (even if restricted to the range $d > \beta^{-1}$), and we regard this agreement as very satisfactory. This also proves that the dispersion on thickness d

TABLE V. The nonlinear susceptibilities d_{22}/ε_0 (in m/V) at 1.06 μm found in various works.

	Akhundov *et al.* 1973 (Ref. 1)	Catalano and co-workers 1979 (Refs. 2 and 3)	This work
GaSe	38.4×10^{-11}	37.3×10^{-11}	8.5×10^{-11}
InSe	8.53×10^{-11}	10.3×10^{-11}	18.5×10^{-11}
Ratio GaSe/InSe	4.5	3.6	0.47

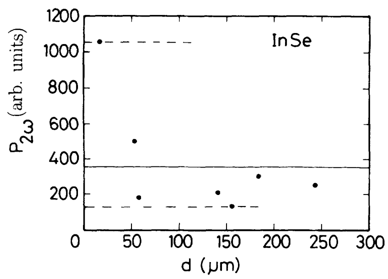

FIG. 4. Transmitted harmonic power output $P_{2\omega}$ as a function of traversed thickness d in InSe, at constant incoming IR power. The dashed lines show the upper and lower limits of $P_{2\omega}$ due to the Fabry-Pérot cavity effect enhanced by laser instability [Eq. (34)]. The solid line indicates the expected output power for a sufficiently rough plate.

over the IR beam cross section is very small in our samples. This is due to the way they have been selected: we have chosen those which exhibited the largest contrast in their transmission spectrum. The measured dynamic range is a little larger than the theoretical one; this enhancement is due to laser instability. If for the measured values of $P_{2\omega}$ we assume

$$P_{2\omega}=P^{\circ}_{2\omega}f(d)(1+\alpha X)^2 , \tag{34}$$

X being a random number ($-1<X<1$) and α a laser instability factor, Figs. 3 and 4 provide $P^{\circ}_{2\omega}$ values of 190 and 337 in arbitrary units, for GaSe and InSe, respectively. The laser instability factor α is found to be 2.5 and 6% respectively, which is quite credible.

In Figs. 3 and 4 the SH output dynamic range is observed to drop for large values of thickness. This is attributable to the increasing sample roughness at large d. A roughness Δd exceeding the half-wavelength (0.19 μm inside the materials) blurs the Fabry-Pérot function $f(d)$, and replaces it by its average $\langle f \rangle \simeq 1.2$. While the layered structure of the III-VI semiconductors certainly helps to ensure thickness uniformity over the laser beam cross section to a subwavelength precision for thin samples, it cannot do the same for thick samples ($d \sim 200-1000$ μm). For the thickest samples, the measured values of $P_{2\omega}$ should therefore be found between two limits, $P^{\circ}_{2\omega}\langle f \rangle(1-\alpha)^2$ and $P^{\circ}_{2\omega}\langle f \rangle(1+\alpha)^2$. For GaSe, these lower and upper limits are 188 and 208 a.u., respectively, whereas the observed value is 200, in agreement with our theory. For InSe, the limits are 314 and 400 a.u., respectively, and the observed value $P_{2\omega}=243$ a.u. does not lie in between. This is easily explained by a slight attenuation ($\beta_\omega=3$ cm^{-1}) of the fundamental wave which multiplies the IR output amplitude by a factor $\exp(-\beta_\omega d)$, and the SH output power by $\exp(-4\beta_\omega d)$. The limits are changed into 235 and 299 a.u., which enclose the observed value. Andriyashik *et al.*[13] report a value $\beta_\omega \simeq 0.5$ cm^{-1} at 1.165 eV (1.064 μm) and 300 K, related to phonon-assisted transitions in the vicinity of the (indirect) energy gap at 1.173 eV. Again we regard the agreement as very satisfactory.

Having checked the theory for each material, we proceed to compare their nonlinear coefficients d', which was the *raison d'être* for this study. In GaSe and InSe, the d' appearing in Eq. (1) is equal to d_{22} in the usual notation.[5] The transmitted SH output power at constant IR input is proportional to $d'^2\phi$ [Eq. (25)], where the dimensionless factor ϕ related to the linear coefficients is given in Table III with $f(d)$ taken to be $\langle f \rangle$. From the previous data (obtained with the same laser beam) we infer

$$d'(\mathrm{GaSe})/d'(\mathrm{InSe})=0.48 ,$$

in striking contrast to previous determinations;[1-3] see Table V. Since the ratio $\phi(\mathrm{GaSe})/\phi(\mathrm{InSe})$ is nearly the same in both treatments, the discrepancy is probably due to the Fabry-Pérot function $f(d)$, which was ignored so far.[1-3] This is very likely in the case of Akhundov *et al.*[1] who refer to a paper by Bloembergen and performed reflected SH power measurements, which are very different according to the treatment; see Table IV. However, the samples of Catalano and co-workers[2,3] were studied by transmission and were rather thick, so that they should have met the condition $f(d)=\langle f \rangle$. Even in the absence of roughness, the highest discrepancy induced by the Fabry-Pérot cavity effect is by a factor of 6.2 in SH power, and this does not suffice to account for the difference between our GaSe/InSe ratio and theirs. Another cause of the discrepancy would lie in fabrication flaws in either material or both, in their case or ours. In this respect it seems that, unlike our samples, their GaSe and InSe samples were grown in different laboratories.[2,3]

In order to obtain the absolute values of d', we have compared the $P_{2\omega} \sim d'^2\phi$ from GaSe, InSe, and GaP. We used a 482-μm-thick GaP wafer purchased from Wacker and polished in one of our laboratories. For linear optical constants, Ref. 14 gives $n_\omega=3.05$ and $n_{2\omega}=3.50$, whereas $\beta=0.25\times10^3$ cm^{-1} was measured in one of our laboratories (Table 2 of Ref. 15); this yields $\phi=0.61\times10^{-2}$. The nonlinear coefficient d_{14}/ε_0 of this material is known[16] to be 1.0×10^{-10} m/V at 1.318 μm, and believed to be more reliable than the former value[17] 0.7×10^{-10} m/V obtained at 1.06 μm. The GaP plate was oriented normally to the $\langle 111 \rangle$ direction and the coefficient d' (GaP) is found to be equal to $2d_{14}/\sqrt{6}$. In moving the sample normal to the laser beam by 120-μm steps, we found oscillations by $\pm25\%$ around the average green light output, that we attribute to thickness fluctuations and Fabry-Pérot ensuing effects. This is consistent with the expected quality of the polishing, which is deemed to give a residual roughness no better than 0.1 μm. Another source of uncertainty (not expected in layered materials) comes from a locally non-normal incidence, which upon average over the beam cross section is expected to reduce the Fabry-Pérot finesses. From Fig. 5, and accounting for the difference between $P_{2\omega}$ (InSe, $d=243$ μm) and $P^{\circ}_{2\omega}\langle f \rangle$, we obtain the ratios for the d' coefficients relative to GaP, for which

$$d'(\mathrm{GaSe})/\varepsilon_0=8.5\times10^{-11}\ \mathrm{m/V}$$

and

$$d'(\mathrm{InSe})/\varepsilon_0=18.5\times10^{-11}\ \mathrm{m/V} ,$$

and the nonlinear susceptibilities d_{22}/ε_0 of GaSe and

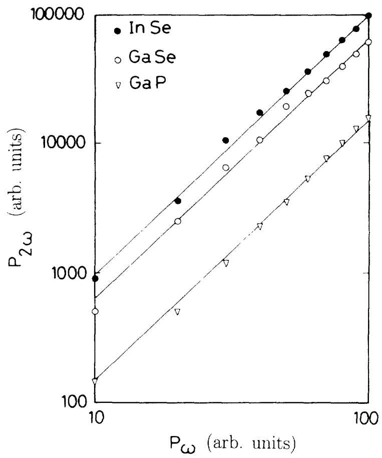

FIG. 5. Harmonic power output $P_{2\omega}$ as a function of input IR power P_ω ($10<P_\omega<100$ mW on average), for GaSe, InSe, and GaP(111). The thicknesses were 518, 243, and 482 μm, respectively. The solid lines are least-square fits to the experimental data, with slope 2 in logarithmic scales.

InSe are reported in Table V. The GaSe/InSe susceptibility ratio from the data of Fig. 5 is 0.46, consistent with the ratio (0.48) derived from Figs. 3 and 4.

V. CONCLUSION

This paper was motivated by the specific behavior of optical materials generating *and* absorbing second-harmonic radiation in the presence of a fundamental wave–and where phase matching between fundamental and SH waves is not necessarily achieved. We have first addressed the simpler case of traveling waves at ω and 2ω, and this has led to the characteristic damping length L of the fundamental beam, scaling as P_ω^{-1}. For a traversed thickness in excess of L, the outgoing power at 2ω ceases to be quadratic, and becomes constant, with respect to the incoming power at ω. In most practical cases, L is extremely large. Second, assuming no depletion of the fundamental wave, we have studied SH generation in a plane-parallel plate of material absorbing the harmonic wave (i.e., of thickness in excess of the attenuation length). We have checked that in the limiting case for indices close to unity, our theory reduces to that of Bloembergen and Pershan.[11] In contrast, a very significant departure is found in high-index materials ($\gtrsim 3$) if thickness is well defined (as is expected in layered III-VI semiconductors). Even if Fabry-Pérot effects are thickness averaged, there remains a departure by a factor of 2.5 in the transmitted SH output power in our examples (Table III). Finally, taking GaSe and InSe at 1.06 μm, we have observed a sample dependence agreeing with our predictions. The application of our theory gives values for GaSe and InSe nonlinear susceptibilities of 1.06 μm, taking GaP as a reference material. The difference with former determinations[1–3] is twofold. (1) The moderate discrepancy between our ($d_{22}/\varepsilon_0=18\times10^{-11}$ m/V) and the previous[3] ($d_{22}/\varepsilon_0=10\times10^{-11}$ m/V) susceptibility of InSe may be ascribed to our propagation theory and/or to the different reference materials. (2) The marked change in the GaSe/InSe susceptibility ratio at 1.06 μm (here 0.47, instead of ~ 4) is partly due to a strong, accidental Fabry-Pérot effect in either semiconductor or both, not accounted for in the previous measurements,[1–3] but a fabricational difference between our and their materials is likely. We shall parenthetically remark that the finding that GaSe and InSe have rather close nonlinear susceptibilities (by a factor of 0.47) is not surprising to us, since our own determination of the band structures of both materials points to a great similarity at the atomic level.[18,19] It is hoped that the present paper will help to determine more accurately the nonlinear susceptibilities of materials in their absorbing range. While practical applications of nonlinear materials in that range are scarce, the knowledge of the nonlinear coefficients is of interest in verifying quantum-electronic theoretical models of nonlinear optical properties.

ACKNOWLEDGMENTS

We are indebted to Ph. de Sandro for information on GaSe, to C. Jauberthie-Carillon for the use of her high-quality GaP sample, and to C. Porte for advice and assistance in polishing the sample. Acoustique et Optique de la Matière Condensée, Université Pierre et Marie Curie is URA 800 du CNRS and Physique des Milieux Condensés, Université Pierre et Marie Curie is URA 782 du CNRS.

APPENDIX A

This appendix is devoted to solving for Eq. (11), determining function $A_\omega(z)$:

$$dA_\omega/dz=-(\kappa^2/\Lambda)A_\omega^*[A_\omega^2(z)-A_\omega^2(0)\exp(-\Lambda z)]\ . \tag{A1}$$

The function $A_\omega(z)=\rho_1(z)\exp[i\theta_1(z)]$ will be separated into its modulus and phase, with $\theta_1(0)=0$. In (A1) for $z\gg 1/|\Lambda|$, we shall neglect the exponential term compared to $\rho_1^2(z)$, of which it will be shown that it decays subexponentially. If the real part β of Λ dominates, such neglect is obvious; in case Λ is dominated by its imaginary part Δk (see Table I), the neglect is due to the rapid phase variation, which gives a negligible contribution to A_ω upon integration of (A1). Let $\Lambda=|\Lambda|e^{i\theta}$, i.e., $tg\theta=\Delta k/\beta$ and $|\Lambda|=(\Delta k^2+\beta^2)^{1/2}$. Then (A1) reads

$$dLn\rho_1/dz+id\theta_1/dz=-(\kappa^2/|\Lambda|)\rho_1^2(z)e^{-i\theta}\ . \tag{A2}$$

By separating the real and imaginary parts, one obtains

$$d\rho_1/dz=-(\kappa^2/|\Lambda|)\rho_1^3(z)\cos\theta\ , \tag{A3a}$$

$$d\theta_1/dz=(\kappa^2/|\Lambda|)\rho_1^2(z)\sin\theta\ . \tag{A3b}$$

The solution of (A3a) can be obtained in a straightforward manner:

$$\rho_1(z)=\rho_1(0)(1+z/L)^{-1/2}\ , \tag{A4}$$

where L denotes $l^2|\Lambda|/(2\cos\theta)=l^2|\Lambda|^2/2\beta$ [Eq. (12)].

Equation (A3b) governing the phase $\theta_1(z)$ can now be solved, by injecting (A4) into (A3b):

$$\theta_1(z)=(\tfrac{1}{2})tg\theta Ln(1+z/L) \ . \tag{A5}$$

For infinite z, the phase varies logarithmically. From the examination of (A4) and (A5), it appears that $A_\omega(z)$ varies with the characteristic length L, and that dA_ω/dz is of the order of A_ω/L, thereby legitimating the integration by parts leading to (A1), since $L \gg |\Lambda|^{-1}$.

Near $z=0^+$, i.e., for $z<1/|\Lambda|$, the aforewritten formulas are not applicable, due to the neglect of the exponential term in (A1). The attenuation-coherence length $|\Lambda|^{-1}$ is a second characteristic transition length, much shorter than L according to our starting hypothesis, so that both crossovers can be treated separately. From (A1) one obtains by evaluating the successive derivatives d^nA_ω/dz^n at $z=0$:

$$A_\omega(z)=\rho_1(0)[1-z^2/2l^2+(\Lambda/6l^2)z^3+o(z^3)] \ , \quad z\to 0^+ \ , \tag{A6a}$$

or, equivalently,

$$\rho_1(z)/\rho_1(0)=1-z^2/2l^2+o(z^2) \quad (z\to 0^+) \ , \tag{A6b}$$

$$\theta_1(z)=(\Delta k/6l^2)z^3+o(z^3) \quad (z\to 0^+) \ . \tag{A6c}$$

The crossover between (A6b) and (A4) takes place for $z^2/2l^2=z/2L$, i.e., $z=2(\cos\theta)/|\Lambda|$. Analogously, the crossover for function $\theta_1(z)$ [Eqs. (A6c) and (A5)] is found to occur at $z=\sqrt{6}/|\Lambda|$. In each case, the length is in the micrometer range (Tables I and II).

Consider now the function $A_{2\omega}(z)$. It is related to $A_\omega(z)$ through Eq. (9a):

$$A_{2\omega}(z)=(-i\kappa/\Lambda)[A_\omega^2(z)e^{\Lambda z}-\rho_1^2(0)] \ . \tag{A7}$$

Using Eqs. (A4) and (A5) for $A_\omega(z)$ yields for the spatial part $E_{2\omega}(z)$ of the electric field ($z\gg\beta^{-1}$):

$$E_{2\omega}(z)=(-i\kappa/\Lambda)\frac{\rho_1^2(0)}{1+z/L} \times\exp[-2ik_\omega z+i\Delta kLn(1+z/L)/\beta] \ . \tag{A8}$$

Expression (A8) warrants a comment. For $z\ll L$, the phase evolution of $E_{2\omega}(z)$ is governed by the wave vector k_ω of the fundamental wave; that is, $E_{2\omega}$ is a forced field which is determined from the undamped fundamental field and varies as E_ω^2; accordingly, the modulus of $E_{2\omega}(z)$ is constant over the region $\beta^{-1}\ll z\ll L$. For $z>L$, an additional phase variation appears which is but logarithmic in z, while the modulus drops as z^{-1}.

The SH output power density at $z=d$ is ($d\gg\beta^{-1}$)

$$P_{2\omega}=(2/\varepsilon_0 c)(\kappa/|\Lambda|)^2P_\omega^2/(1+d/L)^2 \tag{A9}$$

and therefore varies quadratically with the input power at ω, independent of d, as long as $d\ll L$. For $\beta d\lesssim 1$, $\rho_1(z)$ is nearly constant, and (A9) is to be multiplied by $|1-e^{-\Lambda d}|^2$, which introduces damped oscillations of period $2\pi/\Delta k$ over the attenuation length. For $\beta^{-1}\ll d\ll L$, Eq. (A9) may be written

$$P_{2\omega}=(|\Lambda|^{-1}/l)^2P_\omega \ . \tag{A10}$$

Because $|\Lambda|^{-1}\ll l$, relation (A10) explicitly shows that the conversion factor is $\ll 1$ (ideal case). Keep in mind that $|\Lambda|^{-1}\ll l$, i.e., $P_\omega\ll(\frac{1}{2})\varepsilon_0 c|\Lambda|^2\kappa^{-2}$, is the condition for the present treatment to be valid.

In the region $0<z<|\Lambda|^{-1}$, the SH radiation grows from zero as $|1-e^{-\Lambda z}|$:$|A_{2\omega}(z)|$ is pseudoperiodic, the oscillations being damped for $z\gg\beta^{-1}$. Then $|A_{2\omega}(z)|$ slowly decays as $(1+z/L)^{-1}$, while the phase of $A_{2\omega}(z)$ oscillates with the spatial period $2\pi/\Delta k$. In the asymptotic region ($z\gg L$), (A9) yields

$$P_{2\omega}=(\tfrac{1}{2})\varepsilon_0 c|\Lambda|^2/(2\kappa\beta d)^2 \ , \tag{A11}$$

so that $P_{2\omega}$ becomes independent of the input power but decreases as the inverse of d^2.

APPENDIX B

This appendix is devoted to obtaining the harmonic transmitted ($E_{\rm out}$) and reflected ($E'_{\rm out}$) fields from the forced harmonic field generated by the fundamental wave and the boundary conditions. The forced 2ω field is given by Eq. (17):

$$E_f(z)=-2\mu_0\omega^2d'E_0^2\left[\frac{\exp(-2ik_\omega z)+r^2\exp[2ik_\omega(z-d)]}{(k_{2\omega}-i\beta)^2-(2k_\omega)^2}+\frac{2r\exp(-ik_\omega d)}{(k_{2\omega}-i\beta)^2}\right] , \tag{B1}$$

to which a free 2ω field is added [Eq. (19)]:

$$b_+\exp[-(ik_{2\omega}z+\beta)z]+b_-\exp[(ik_{2\omega}+\beta)(z-d)] \ . \tag{B2}$$

The harmonic field in vacuum is [Eqs. (20a) and (20b)]:

$$E_{2\omega}(z)=E_{\rm out}\exp[-2i\omega(z-d)/c] \quad (z>d) \ , \tag{B3}$$

$$E_{2\omega}(z)=E'_{\rm out}\exp(2i\omega z/c) \quad (z<0) \ . \tag{B4}$$

We are left with four unknowns $E_{\rm out}$, $E'_{\rm out}$, b_+, and b_-. For normal incidence the electric and magnetic fields are parallel to the boundaries and continuous at $z=0$ and d. Continuity of $E_{2\omega}$ entails

$$E'_{\rm out}=E_f(0)+b_++b_-\exp[-i(k_{2\omega}-i\beta)d] \ , \tag{B5}$$

$$E_{\rm out}=E_f(d)+b_+\exp[-i(k_{2\omega}-i\beta)d]+b_- \ . \tag{B6}$$

Continuity of the harmonic magnetic field gives two more equations:

$$E'_{\rm out}=2n_\omega\mu_0\omega^2 d' E_0^2\left[\frac{1-r^2\exp(-2ik_\omega d)}{(k_{2\omega}-i\beta)^2-(2k_\omega)^2}\right.$$
$$\left.+\tilde{n}_{2\omega}\{b_+-b_-\exp[-i(k_{2\omega}-i\beta)d]\}\right] , \tag{B7}$$

$$E_{\rm out}=-2n_\omega\mu_0\omega^2 d' E_0^2\left[\frac{\exp(-2ik_\omega d)-r^2}{(k_{2\omega}-i\beta)^2-(2k_\omega)^2}\right.$$
$$\left.+\tilde{n}_{2\omega}\{b_+\exp[-i(k_{2\omega}-i\beta)d]-b_-\}\right] . \tag{B8}$$

If, in Eqs. (B5) and (B6), βd is taken to be $\gg 1$, then

$$b_+=E'_{\rm out}-E_f(0) , \tag{B9}$$

$$b_-=E_{\rm out}-E_f(d) . \tag{B10}$$

Similarly, one term may be dropped in (B7) and (B8) if $\beta d \gg 1$. Injection of (B9) into the simplified (B7), and of (B10) into the simplified (B8), yields decoupled expressions for $E_{\rm out}$ and $E'_{\rm out}$. The expressions are Eqs. (22a) and (22b). Thus we see that if $d \gg \beta^{-1}$, both boundaries behave independently. At each interface the forced wave (with wave vector $2k_\omega$) generates a free wave (of wave vector $k_{2\omega}$) in the nonlinear medium, together with an outgoing wave in vacuum, in order to satisfy the boundary condition. The interface at $z=0$ generates a forward-traveling free wave which damps at $z \gg \beta^{-1}$. The interface at $z=d$ generates a backward-traveling free wave which vanishes for $d-z \gg \beta^{-1}$. Inside the plate of thickness $d \gg \beta^{-1}$ those two free waves do not overlap, so that the boundaries ignore each other.

[1]G. A. Akhundov, A. A. Agaeva, V. M. Salmanov, Yu. P. Sharonov, and I. D. Yaroshetskii, Fiz. Tekh. Poluprovodn. 7, 1229 (1973) [Sov. Phys. Semicond. 7, 826 (1973)].

[2]I. M. Catalano, A. Cingolani, A. Minafra, and C. Paorici, Opt. Commun. **24**, 105 (1978).

[3]I. M. Catalano, A. Cingolani, C. Cali, and S. Riva-Sanseverino, Solid State Commun. **30**, 585 (1979).

[4]A. Bourdon, E. Bringuier, M. T. Portella, M. Vivières, and N. Piccioli, Phys. Rev. Lett. **65**, 1925 (1990).

[5]Amnon Yariv, *Quantum Electronics,* 2nd and 3rd eds. (Wiley, New York, 1975 and 1987). A factor of 2 in the nonlinear term has been corrected in the latest edition.

[6]J. A. Armstrong, N. Bloembergen, J. Ducuing, and P. S. Pershan, Phys. Rev. **127**, 1918 (1962).

[7]R. Le Toullec, N. Piccioli, M. Mejatty, and M. Balkanski, Nuovo Cimento **38B**, 159 (1977).

[8]N. Piccioli, R. Le Toullec, F. Bertrand, and J.-C. Chervin, J. Phys. (Paris) **42**, 1129 (1981).

[9]G. L. Harris, E. W. Jones, M. G. Spencer, and K. H. Jackson, Appl. Phys. Lett. **59**, 1817 (1991).

[10]R. S. Craxton, IEEE J. Quantum Electron. **QE-17**, 1771 (1981).

[11]N. Bloembergen and P. S. Pershan, Phys. Rev. **128**, 606 (1962).

[12]S. K. Kurtz, in *Quantum Electronics: A Treatise,* edited by Herbert Rabin and C. L. Tang (Academic, New York, 1975), Vol. 1, Part A, pp. 209–281.

[13]M. V. Andriyashik, M. Y. Sakhnoskii, V. B. Timofeev, and A. S. Yakimova, Phys. Status Solidi **28**, 277 (1968); see also A. Segura Garcia del Rio, Ph.D. thesis, Université Pierre et Marie Curie, Paris, 1977, pp. 11 and 12.

[14]D. E. Aspnes and A. A. Studna, Phys. Rev. B **27**, 985 (1983).

[15]C. Jauberthie-Carillon and C. Guillemin, J. Phys. Condens. Matter **1**, 6807 (1989).

[16]B. F. Levine and C. G. Bethea, Appl. Phys. Lett. **20**, 272 (1972).

[17]R. C. Miller, Appl. Phys. Lett. **5**, 17 (1964).

[18]A. Bourdon, J. Phys. (Paris) **35**, C3-261 (1974).

[19]A. Bourdon, A. Chevy, and J. M. Besson, in *Physics of Semiconductors 1978* (Edinburgh, Scotland, 4–8 Sept. 1978), edited by B. L. W. Wilson, IOP Conf. Proc. No. 43 (Institute of Physics and Physical Society, London, 1979), pp. 1371–1374.